

CrossMark  
click for updatesCite this: *RSC Adv.*, 2016, 6, 107689

# Benzoxazines with enhanced thermal stability from phenolated organosolv lignin

Ghizelle Jane Abarro,<sup>†ab</sup> Jacob Podschun,<sup>†c</sup> Leslie Joy Diaz,<sup>b</sup> Seishi Ohashi,<sup>a</sup> Bodo Saake,<sup>c</sup> Ralph Lehnen<sup>d</sup> and Hatsuo Ishida<sup>\*a</sup>

Lignin-based benzoxazines are synthesized for the first time using organosolv lignin as the phenolic component and aniline or propargyl amine as the amine component through the Mannich condensation reaction. Acid-catalyzed phenolation of organosolv lignin is performed to increase the phenolic structure with the open *ortho*-position, which is a requirement for an oxazine ring formation. Two model compounds using *o*-cresol and *p*-cresol as the phenolic component and propargylamine as the amine component are also synthesized for comparison. The successful syntheses are verified by Fourier transform infrared spectroscopy (FT-IR); proton, carbon and phosphorus nuclear magnetic resonance spectroscopy (<sup>1</sup>H, <sup>13</sup>C and <sup>31</sup>P NMR); and elemental analysis. Further structural characterization of the precursor resins is performed using heteronuclear single quantum coherence (HSQC) NMR technique. The polymerization process is followed by both differential scanning calorimetry (DSC) and *in situ* isothermal FT-IR technique. The polymerization of the lignin-based benzoxazines proceeds faster than ordinary benzoxazine monomers due to the catalytic effect of the residual phenolic moieties in the lignin units. The majority of polymerization process takes place in less than 15 min at 180 °C for both lignin-based benzoxazines studied. The thermal stability of the polymers under study is evaluated by thermogravimetric analysis (TGA). The char yields of the polybenzoxazines derived from the lignin-based benzoxazines are close to 50%, which lead to LOI values considered self-extinguishing.

Received 6th September 2016  
Accepted 28th October 2016

DOI: 10.1039/c6ra22334f

www.rsc.org/advances

## 1 Introduction

Efforts to shift dependence from petroleum-based feedstock target the use of biofuels (bioethanol and biodiesel) as possible alternatives amongst others; yet the high production costs have rendered it underutilized. To address the lack of economical competitiveness, great focus is given to possible value-added applications. The wealth of reactive moieties in lignin's structure makes it a good candidate in the search for renewable feedstocks for polymer production.<sup>1</sup> However, the utility of lignin remains limited owing to the variability of its molecular structure, which depends on geographic origin,<sup>2,3</sup> phylogenetics,<sup>4</sup> plant morphology<sup>5,6</sup> and isolation method.<sup>7</sup>

Polybenzoxazine is a recently commercialized polymer with wide applicability and favorable properties.<sup>8</sup> When utilizing lignin for benzoxazine synthesis, a proposed method is to break

down lignin into benzenes or phenols for polymer synthesis.<sup>9</sup> One problem however, is that the products obtained were mostly mixtures of isomers and complete conversion into pure compounds is still a curiosity.<sup>10</sup> An alternative approach is the direct conversion of the aromatic hydroxyl groups in the lignin molecule to benzoxazines. However, high contents of syringyl units and low concentrations of *p*-hydroxyphenyl units<sup>7</sup> hinder conversion into high density of benzoxazines and thus prohibit an extended polybenzoxazine formation. Benzoxazine can flexibly be synthesized from almost any kind of phenolic derivatives and primary amine as long as the phenolic structure possesses an unsubstituted *ortho* position. However, due to this lack of phenolic structure with open *ortho* position, lignin was rarely considered as direct building block.<sup>11</sup> This flexibility however appealed to the use of other renewable materials. Benzoxazine monomers have been derived from bio-based phenolic substances such as vanillin from the vanilla orchid,<sup>12</sup> cardanol from cashew nut shell,<sup>13</sup> terpene from orange rind,<sup>14</sup> and urushiol from poison ivy.<sup>15</sup> Recently, Podschun *et al.*<sup>16</sup> presented the acid-catalyzed phenolation of beech organosolv lignin to yield an activated lignin with a multitude of phenolic groups having two free *ortho* sites (Fig. 1, step 1). By this means, lignin could function as the backbone of the benzoxazine.

Recently, the overall compatibility of lignin with polybenzoxazines has been studied. In 2012, blends of lignin with

<sup>a</sup>Department of Macromolecular Science and Engineering, Case Western Reserve University, Cleveland, Ohio 44106-7202, USA. E-mail: hxi3@case.edu; Tel: +1 216 368 4285

<sup>b</sup>Department of Mining, Metallurgical and Materials Engineering, University of the Philippines, Diliman, Quezon City, Philippines

<sup>c</sup>Department of Wood Science and Chemical Wood Technology, University of Hamburg, Leuschnerstraße 91b, 21031 Hamburg, Germany

<sup>d</sup>Thünen Institute of Wood Research, Leuschnerstraße 91b, 21031 Hamburg, Germany

† These authors contributed equally.



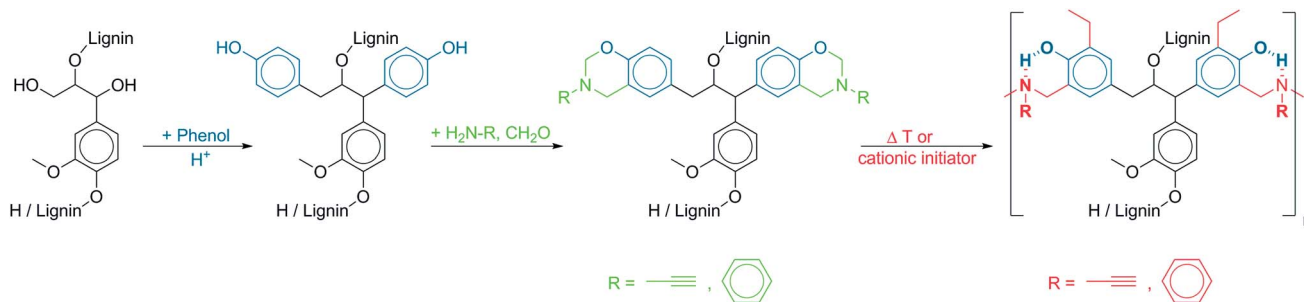


Fig. 1 Phenolation, benzoxazine synthesis and subsequent polymerization to polybenzoxazine with intramolecular six-membered ring of hydrogen bonds.

benzoxazine resin were studied by El Mansouri *et al.* and Haque *et al.*<sup>17,18</sup> Both groups observed that higher amounts of lignin led to lower polymerization temperatures ( $T_p$ ) and higher glass-transition temperatures ( $T_g$ ) but at the expense of phase homogeneity.<sup>18</sup> Lignin also improved the char yield, an indicative parameter of flame retardance. Upon calculation of the limiting oxygen index, the blend material was classified as self-extinguishing.<sup>17</sup> Ougi *et al.* filed a patent on a lignin compound, in which the phenolic structures were converted into benzoxazine moieties. Sufficient free reactive aromatic *ortho* positions were achieved by mixing the new compound with a phenolic resin in a blend.<sup>19</sup> In 2013, Chiou and Ishida suggested that such method resulting in coexistence of lignin and benzoxazine on the same molecule might amplify the benefits reported by El Mansouri *et al.* and Haque *et al.*<sup>11</sup> Later on that year, Comí *et al.* reported synthesis of benzoxazines from phenolic compounds that resemble the lower molecular weight substructures in lignin.<sup>20</sup> The lack of phenolic structures with unsubstituted *ortho* position in naturally derived lignin decomposition products rendered this approach limited success since free *ortho* positions only constitute a small fraction of total phenolic structures.

In order to overcome this difficulty, this study explores the effects of forming more benzoxazine moieties in the lignin structure by using phenolated beech organosolv lignin (PL), which contained the highest values of reactive functionalities among lignins studied.<sup>21</sup> Aniline (abbr. a, Fig. 1, step 2) was chosen as it is a commonly used amine component for most basic benzoxazines. Additionally, the more reactive propargylamine (abbr. pgl, Fig. 1, step 2), which forms a stable aromatic structure upon crosslinking, was investigated to study potential synergistic effects that may result with lignin. The thermal behavior of both lignin-based benzoxazines (aniline and propargyl-based benzoxazines are hereinafter abbreviated as PL-a and PL-pgl, respectively) was compared to two model compounds based on *p*- and *o*-cresols to resemble *p*- and *o*-monosubstituted phenol attached to lignin.

Thus the biopolymer lignin could potentially be equipped with the interesting properties of benzoxazines, namely, that they polymerize without the aid of harsh catalysts and do not produce volatile organic compounds. Furthermore, benzoxazine resins usually show near-zero volume shrinkage during polymerization, low water absorption, glass transition temperature much higher than polymerization temperature, excellent

heat resistance and flame retardance, fast mechanical property development at low crosslinking levels, and very low surface energy.<sup>22–25</sup> These advantageous properties result in various high-performance applications in fields such as aerospace, electronics, and composites.<sup>8</sup>

The abovementioned characteristics are common to all poly-benzoxazines because of the benzoxazine unit, which upon polymerization forms a six-membered ring due to intramolecular hydrogen bonds between the phenolic OH group and the nitrogen atom of the tertiary amine in polybenzoxazine (Fig. 1, step 3).

## 2 Experimental

### 2.1 Extraction and phenolation of lignin

Beech organosolv lignin was produced and phenolated according to our previous publication.<sup>16</sup> Phenolation conditions applied included: phenol (20 g, 0.21 mol), lignin (10 g, ~0.05 mol C<sub>9</sub> units), H<sub>2</sub>SO<sub>4</sub> (1.1 mL, 0.02 mol),  $T = 110\text{ }^\circ\text{C}$ ,  $t = 20\text{ min}$ . The phenolated lignin (PL) was determined to contain 4.3 mmol g<sup>-1</sup> phenol attached to lignin.

### 2.2 Synthesis of benzoxazines based on phenolated lignin and aniline (PL-a) or propargylamine (PL-pgl)

In a 25 mL round bottom flask, the amine (a: 786  $\mu\text{L}$ , pgl: 550  $\mu\text{L}$ , 8.6 mmol) was reacted with paraformaldehyde (516 mg, 17.2 mmol) in 1 mL toluene-ethanol (1 : 1, by vol) for 15 min under nitrogen atmosphere at 95  $^\circ\text{C}$  to form a clear solution. 1 g phenolated lignin (PL) completely dissolved in 4 mL toluene-ethanol (1 : 1, by vol) was added. The reaction was proceeded at 95  $^\circ\text{C}$  under reflux and nitrogen atmosphere for 20 h. After cooling to r.t., the lignin-benzoxazines were precipitated by adding 50 mL diethyl ether. The solids were collected on cellulose acetate membrane, washed with 200 mL diethyl ether, and dried under vacuum to obtain light-brown powders in yields of 1.24 g (82%) for PL-a, and 1.00 g (78%) for PL-pgl.

### 2.3 Synthesis of the propargylamine-based model compounds (*o*C-pgl and *p*C-pgl)

The two model compounds used in this study were 8-methyl-3-(prop-2-yn-1-yl)-3,4-dihydro-2*H*-benzo[*e*][1,3]oxazine and 6-methyl-3-(prop-2-yn-1-yl)-3,4-dihydro-2*H*-benzo[*e*][1,3]oxazine,



which were derived from the reaction of propargylamine with *o*-cresol and *p*-cresol (*o*C-pgl and *p*C-pgl, respectively). The following were added in a 25 mL round bottom flask: *p*-cresol/*o*-cresol (2.42 g, 22 mmol), propargylamine (1.43 mL, 22 mmol), paraformaldehyde (1.35 g 45 mmol), and toluene (5.19 mL, 49 mmol) as solvent. The mixture was heated under reflux at 95 °C for 3 h. Both products were washed three times with 3 N NaOH to remove unreacted phenols; and three times with distilled water to remove residual NaOH in the solution. The product was dried with anhydrous sodium sulfate and filtered. Toluene was removed by air blowing for 24 h followed by drying at 50 °C in a vacuum oven for 24 h. Both were obtained as clear fluids with *o*C-pgl being colorless and *p*C-pgl having a yellowish color. The yields were 88% and 95%, respectively.

<sup>1</sup>H NMR  $\delta$  (300 MHz, ppm, CDCl<sub>3</sub>): *o*C-pgl: 2.24 (Ar-CH<sub>3</sub>), 2.40 ( $\equiv$ CH), 3.62 (-CH<sub>2</sub>-), 4.14 (Ar-CH<sub>2</sub>-N), 4.98 (O-CH<sub>2</sub>-N) and 6.86–7.04 (Ar-H). *p*C-pgl: 2.27 (Ar-CH<sub>3</sub>), 2.33 ( $\equiv$ CH), 3.60 (-CH<sub>2</sub>-), 4.09 (Ar-CH<sub>2</sub>-N), 4.91 (O-CH<sub>2</sub>-N), and 6.72–6.97 (Ar-H).

## 2.4 Equipments and characterization

**NMR (nuclear magnetic resonance) spectroscopy of lignin compounds.** NMR (nuclear magnetic resonance) spectroscopy of lignin compounds was performed on a Bruker Avance III HD 400 MHz spectrometer equipped with a BBFO probe with *z*-gradient. Processing of one-dimensional NMR spectra was performed with ACD/Labs NMR processor (version 12, lb = 3 Hz for <sup>13</sup>C and <sup>31</sup>P spectra, phase and baseline correction, DMSO as internal reference at  $\delta_c$  39.5 ppm and  $\delta_H$  2.50 ppm).

**<sup>1</sup>H NMR.** <sup>1</sup>H NMR spectra of lignin samples (about 25 mg) were recorded in 0.6 mL DMSO-d<sub>6</sub> containing 3 mg mL<sup>-1</sup> of hexamethylcyclotrisiloxane as internal standard. Acquisition parameters included: 40 °C, 6006 Hz spectral window, 128 scans, 2 s acquisition time and 10 s delay between pulses.

**<sup>31</sup>P NMR.** <sup>31</sup>P NMR spectroscopy was performed following a published procedure.<sup>26</sup> Phosphitylation was performed with 2-chloro-4,4,5,5-tetramethyl-1,3,2-dioxaphospholane and *endo-N*-hydroxyl-5-norbornene-2,3-dicarboximide was used as IS.<sup>27</sup> Acquisition parameters included: 25 °C, 11 990 Hz spectral window, 256 scans, acquisition time 1.0 s and a 20 s delay between pulses.

**<sup>13</sup>C NMR.** <sup>13</sup>C NMR spectra were measured adapting a protocol from Capanema *et al.*<sup>28</sup> The lignin sample (130 mg) was dissolved in 0.65 mL DMSO-d<sub>6</sub> followed by the addition of 2.3 mg of chromium(III)acetylacetonate as relaxation agent. Acquisition parameters included: inverse gated decoupling, 40 °C, 25 000 Hz spectral window, 20 000 scans, 1.4 s acquisition time and 2.0 s delay between pulses.

**<sup>1</sup>H <sup>13</sup>C HSQC (heteronuclear single quantum coherence) NMR.** <sup>1</sup>H <sup>13</sup>C HSQC (heteronuclear single quantum coherence) NMR spectra were recorded according to Tran *et al.*<sup>29</sup> The Bruker standard pulse sequence hsqcetgpsp.3 was used with an acquisition time of 170 ms, an interscan delay of 1 s and a d4 delay of 1.8 ms (1/4J, <sup>1</sup>J<sub>CH</sub> = 140 Hz). The spectrum was processed using a squared cosine bell in both dimensions and linear prediction (24 coefficients) in F1 using MestReNova (version 9.1).

**<sup>1</sup>H NMR spectroscopy of model compounds.** <sup>1</sup>H NMR spectroscopy of model compounds was done with a Varian Oxford AS300 with proton frequency of 300 MHz. The solvent and internal standard utilized was deuterated chloroform (CDCl<sub>3</sub>) and tetramethylsilane (TMS), respectively. For integrated intensity measurements, the relaxation time was set at 10 s with an average of 16 transients.

Signal assignments in NMR spectroscopy referred to the literature.<sup>16,30</sup>

**Elemental analysis.** Elemental analysis was accomplished using an Elementar vario EL cube. The elements C, H, N, and S were measured in duplicate. The remaining percentage was associated to oxygen.

**Size exclusion chromatography.** Size exclusion chromatography (SEC) was conducted using a set of three PolarGel-M columns (Agilent, two 7.5 × 300 mm columns and a 7.5 × 50 mm guard column) and DMSO with 0.1% LiBr as eluent. Samples were dissolved (*c* = 1 mg mL<sup>-1</sup>) and shaken in the eluent for 24 h at room temperature. The flow rate was 0.5 mL min<sup>-1</sup> at 60 °C. Glucose and polyethylene glycol standards (180–82 250 g mol<sup>-1</sup>, Agilent) were applied for calibration of the RI detector (RI 71, Shodex). Sample detection was performed using an UV detector (UV-2077, Jasco) at 280 nm, and phenol red was used to match detectors. The data was recorded and evaluated using WinGPC Unichrom V8.10 software from polymer standards service.

**Fourier transform infrared spectroscopy.** Fourier transform infrared spectroscopy (FT-IR) was applied for further structural analysis using a Bomem Michaelson MB 110 spectrophotometer with deuterated triglycine sulfate detector. Samples and background were measured with a KBr plate (300 mg, 7 MPa pressing) by applying the liquid sample onto the KBr plate or by mixing the solid sample (<1 mg) with KBr prior to pressing. 64 scans were accumulated at a resolution of 4 cm<sup>-1</sup>.

For *in situ* FT-IR, the samples were heated to 180 °C by purging with dry air. Starting from room temperature, the target temperature was reached within 10 min. Spectra were recorded at 0, 5, 10, 15, 30, 60, 180 min isothermally.

**Differential scanning calorimetry.** Differential scanning calorimetry (DSC) was performed on a TA Instrument DSC Model 2920. Few milligrams of the samples were enclosed in crimped hermetic aluminum pans. All DSC tests were done with a heating ramp rate of 10 °C min<sup>-1</sup> and a nitrogen flow rate of 60 mL min<sup>-1</sup>. To investigate the thermal behavior of PL, the sample was dried for 48 hours under vacuum. Sample was subjected to three heating runs, allowing the sample to cool to room temperature in between runs. The glass transition temperature was obtained as the peak of the heat capacity curve during the second and third run.

**Thermogravimetric analysis.** Thermogravimetric analysis (TGA) was applied to characterize the thermal stability of PL and polymerized samples using a TA Instruments Model High-Res TGA 2950. Approximately 3 mg of each sample was used with heating ramp rate set to 10 °C min<sup>-1</sup> and a nitrogen flow rate of 60 mL min<sup>-1</sup>. For the purpose of this study, the char yield was defined as the percent residual weight of a material at 800 °C under nitrogen atmosphere.



### 3 Results and discussion

#### 3.1 Thermal properties of phenolated organosolv lignin (PL)

The thermal properties of the phenolated lignin evaluated by DSC (Fig. 2) showed a transition at 107 °C, which was hypothesized to be a glass transition. The second transition event was observed at 251 °C. Previous studies that reported the same observation linked such events with the occurrence of softening in amorphous and semi-crystalline polymers.<sup>31</sup> Both, glass transition and softening, were reversible phenomena and were retained in the third heating run at 107 °C and 251 °C, respectively. Since the energies absorbed were very low, they were not expected to significantly affect thermoset polymerization.

The thermogravimetric analysis in Fig. 3 shows a wide temperature range, at which PL decomposes. This is usually related to the presence of various oxygen-containing functional groups decomposing at different temperatures. Decomposition began at 297 °C, which is associated with the degradation of the propanoid portion to form methyl-, ethyl-, and vinyl-compounds.<sup>32</sup> It continued towards a maximum decomposition temperature of 358 °C as the lignin structure was progressively broken down and weakly bonded groups volatilized.<sup>33–35</sup> However, these degradation products were partially free radicals that either react with each other or with non-degraded lignin *via* radical–radical interactions or electron transfer.<sup>36,37</sup> Such reactions result in heavier intermediate compounds and even rearrangement of the backbone to form char.<sup>38</sup> The char yield of PL at 800 °C was 17.3%, which was slightly higher than that of the unmodified lignin material with a char yield of 15.8%. The increased char yield might be due to the higher content of aromatic structures in PL available for char formation.

#### 3.2 Synthesis and structural characterization of lignin-based benzoxazines

The initial stage of synthesis proceeds by a low-temperature Mannich condensation of the amine component and formaldehyde. This reaction results in a hemiaminal intermediate that forms a perhydrotriazine-ring.<sup>39–41</sup> Upon opening of the

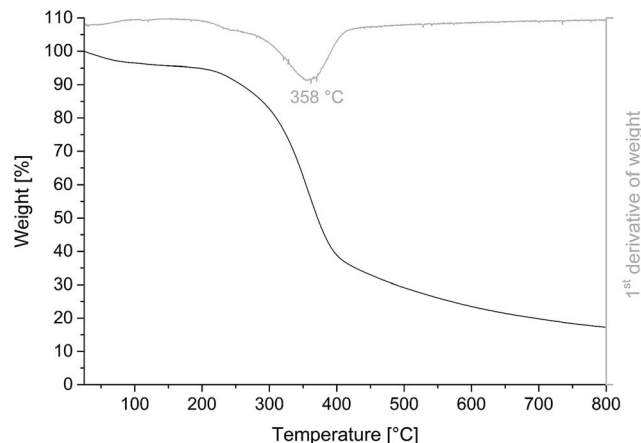


Fig. 3 TGA thermogram of phenolated lignin PL including 1<sup>st</sup> derivative of weight (gray).

perhydrotriazine ring, it reacts with the phenols in PL to form an oxazine ring structure (Fig. 1, step 2).

The hydroxyl groups of both products PL-a and PL-pgl were compared to those of PL by <sup>31</sup>P NMR spectroscopy (Fig. 4). All signal intensities below 141.4 ppm were largely reduced. Especially, the signals at 138.0 ppm referring to *para*-attached phenol units in PL and at 139.6 ppm referring to guaiacyl units almost quantitatively vanished. From the original integrals of PL for *ortho*- and *para*-attached phenol and guaiacyl (4.7 mmol g<sup>-1</sup>) only 0.7 mmol g<sup>-1</sup> for PL-a and 1.1 mmol g<sup>-1</sup> for PL-pgl remained. It was consequently deduced that the majority of active phenolic hydroxyl groups in PL were converted to benz-oxazines. The integrals of signals for aliphatic hydroxyls, 5-substituted moieties and carboxyl groups displayed marginal reduction (PL: 0.2/1.5/0.0; PL-a: 0.1/1.2/0.0; PL-pgl: 0.2/1.3/0.0 mmol g<sup>-1</sup> respectively), potentially related to the mass increase after benzoxazine formation. However, an additional

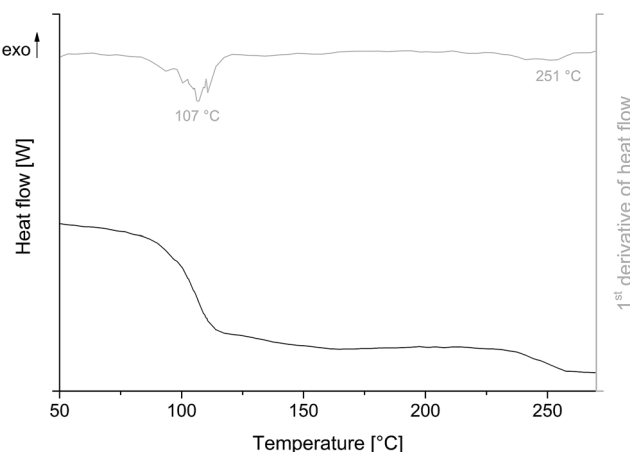


Fig. 2 DSC thermogram of phenolated lignin PL including 1<sup>st</sup> derivative of heat flow (gray).

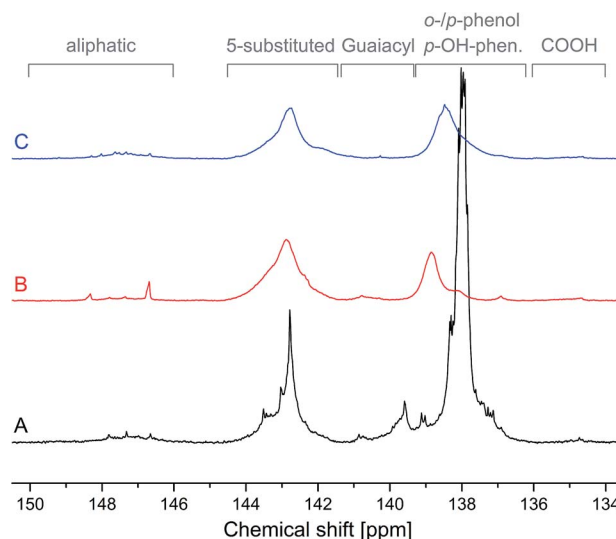


Fig. 4 <sup>31</sup>P NMR spectra of phenolated lignin PL (A), and resulting benzoxazines PL-a (B) and PL-pgl (C) normalized on IS at 151.9 ppm.



peak at 138.8 ppm (PL-a) and 138.5 ppm (PL-pgl) was present. Being present in both products at similar chemical shifts, these peaks signified either an aromatic hydroxyl group or an amino group. However, aromatic and aliphatic amino groups (from aniline and propargylamine) show larger chemical shift separations than that observed.<sup>42</sup> Therefore, these additional peaks were attributed to the unreacted *ortho*-phenols in lignin. The <sup>31</sup>P NMR spectra indicated that in addition to the conversion of nearly all *p*-hydroxyphenyl-equivalent structures to benzoxazines, guaiacyl units were also converted. These results underline that benzoxazine formation proceeded *via* aromatic substitution to etherification/ring closure with the hydroxyl group as it appeared that only hydroxyl groups with free *ortho* sites reacted (not the 5-substituted units).

The structure of the PL-derived benzoxazines was further characterized *via* <sup>1</sup>H/<sup>13</sup>C HSQC NMR. The resonances for PL-pgl were found to overlap in one-dimensional NMR spectra, but could partially be resolved in HSQC spectra. In Fig. 5, the spectra for both lignin–benzoxazines were compared with the spectrum of PL. For PL-a, new signals were observed at 4.6/48.9 ppm and 5.4/78.2 ppm; and for PL-pgl at 3.9/48.6 ppm and 4.8/80.3 ppm. These peaks referred to the methylene groups in the benzoxazine ring (Ar–CH<sub>2</sub>–N and O–CH<sub>2</sub>–N, respectively).<sup>30</sup> The separation of approximately 0.8 and 0.9 ppm between these <sup>1</sup>H resonances was similar to many other benzoxazines in literature, where separation frequencies in the range of 0.8–0.9 ppm were reported.<sup>8</sup> The ratio of integrated peak intensity in the spectra was 1.01 ( $\delta_{4.6/48.9 \text{ ppm}}/\delta_{5.4/78.2 \text{ ppm}}$ ) for PL-a and 0.93 ( $\delta_{3.9/48.6 \text{ ppm}}/\delta_{4.8/80.3 \text{ ppm}}$ ) for PL-pgl. The integrals for PL-a were verified by <sup>13</sup>C NMR (ratio: 1.02, Fig. 6) and <sup>1</sup>H NMR (ratio: 0.99). Integration for PL-pgl was not performed due to overlapping signals (Fig. 5 and 6). Based on these NMR analyses, the formation of the benzoxazine structures was apparent in both samples. For PL-pgl, two additional signals at 3.5/39.6 ppm and 3.2/74.9 ppm arose, representing the methylene and methylidyne group in propargylamine, respectively.<sup>30</sup> Peaks assigned to PL side chain and methoxyl groups remained with reduced intensities.<sup>16</sup> The cross-resonances between 6.6/106.3 ppm and 7.3/129 ppm increased for PL-a, representing aromatic C–H

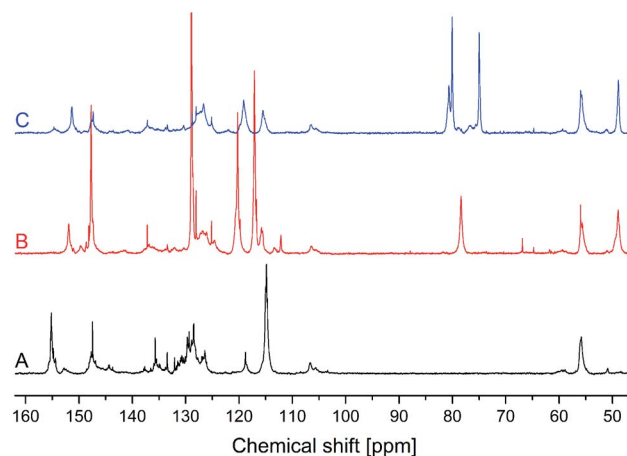


Fig. 6 <sup>13</sup>C NMR of phenolated lignin PL (A) and resulting benzoxazines PL-a (B) and PL-pgl (C).

from aniline attached. For PL-pgl, the resonances of aromatic C–H, especially between 6.5 and 7.3 ppm, decreased due to aromatic substitution of free *ortho* positions.<sup>16</sup>

Besides the two-dimensional cross peaks, new quaternary carbons were identified in <sup>13</sup>C NMR (Fig. 6). These included peaks at 80.1 ppm of the quaternary C in the propargyl group, at 115.7 ppm of C<sub>phenol</sub>–CH<sub>2</sub>–N, at 151.8 ppm of C<sub>1phenol</sub> in PL-a, at 151.4 ppm of C<sub>1phenol</sub> in PL-pgl and at 147.8 ppm of C<sub>1anilin</sub> in PL-a. The original signal at 155.1 ppm of C<sub>1phenol</sub> in PL nearly quantitatively vanished in PL-a and PL-pgl.

The two model compounds are in agreement with the analytical data described by Nagai *et al.*,<sup>30</sup> whose NMR chemical shifts just slightly varied in <sup>13</sup>C NMR due to change in solvent. The amounts of benzoxazine moieties formed were estimated by <sup>1</sup>H NMR spectroscopy with internal standard to be 2.0 mmol g<sup>-1</sup> for PL-a and 2.1 mmol g<sup>-1</sup> for PL-pgl using the peak at  $\delta = 5.4$  ppm and 4.8 ppm, respectively (<sup>1</sup>H traces in Fig. 5).

The incorporation of the amine compounds was examined by elemental analysis. The nitrogen contents measured were 4.5% (3.2 mmol g<sup>-1</sup>) for PL-a, and 4.1% (2.9 mmol g<sup>-1</sup>) for PL-

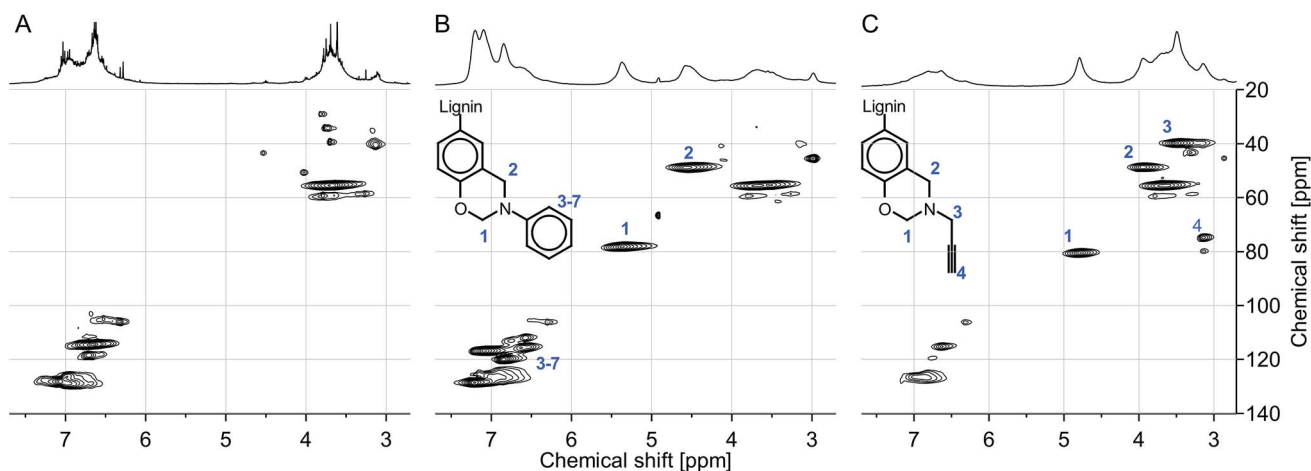


Fig. 5 <sup>1</sup>H/<sup>13</sup>C-HSQC spectra of phenolated lignin PL (A) and resulting benzoxazines PL-a (B) and PL-pgl (C) with <sup>1</sup>H NMR traces.



pgl. The theoretical nitrogen content for complete conversion could be approximated based on the benzoxazines unit molar mass (PL-a:  $119.2 \text{ g mol}^{-1}$ , PL-pgl:  $81.1 \text{ g mol}^{-1}$ ), which adds to the phenolic hydroxyl group of PL (*p*-hydroxyphenyl + guaiacyl:  $4.3 + 0.4 \text{ mmol g}^{-1}$ ) to yield  $3.0 \text{ mmol g}^{-1}$  for PL-a and  $3.4 \text{ mmol g}^{-1}$  for PL-pgl. Thus, theoretical and experimental values for nitrogen contents were in close agreement. However, lower values were obtained from  $^1\text{H}$  NMR quantification, indicating that some nitrogen moieties were otherwise included into the products, besides benzoxazine structures.

In the FT-IR analysis shown in Fig. 7, the lignin-benzoxazines PL-a and PL-pgl are compared to the phenolated lignin PL and two model compounds *o*C-pgl and *p*C-pgl (benzoxazines based on *ortho*- and *para*-cresol, respectively and propargylamine). In this analysis, the obvious appearance of the band around  $940 \text{ cm}^{-1}$  is further evidence of the benzoxazine formation as it corresponds to the out-of-plane bending of a benzene ring with an oxazine ring attached. For propargylamine-based benzoxazines, the appearance of a sharp peak around  $3283 \text{ cm}^{-1}$  and  $645 \text{ cm}^{-1}$  confirmed the attachment of acetylene groups in the structures.<sup>43,44</sup> Traces of paraformaldehyde would also occur near this band as well, but such possibility was discarded since additional paraformaldehyde bands (e.g. at  $1093 \text{ cm}^{-1}$ ) were absent.<sup>45</sup> Other bands in the benzoxazine spectra can be seen at  $1227 \text{ cm}^{-1}$  (Ar-O-C asymmetric stretch),  $1029 \text{ cm}^{-1}$  (Ar-O-C symmetric stretch),  $1328 \text{ cm}^{-1}$  ( $\text{CH}_2$  wagging of oxazine), and  $2750\text{--}3050 \text{ cm}^{-1}$  ( $\text{CH}_2$  stretch of methylene).<sup>8</sup> However, these bands also occurred in PL, though with different intensities. Nevertheless, the large broad peak corresponding to phenols in PL ( $3150\text{--}3600 \text{ cm}^{-1}$ ) apparently decreased for both PL-a and PL-pgl signifying the reaction of phenols to form benzoxazine moieties.<sup>8,45</sup>

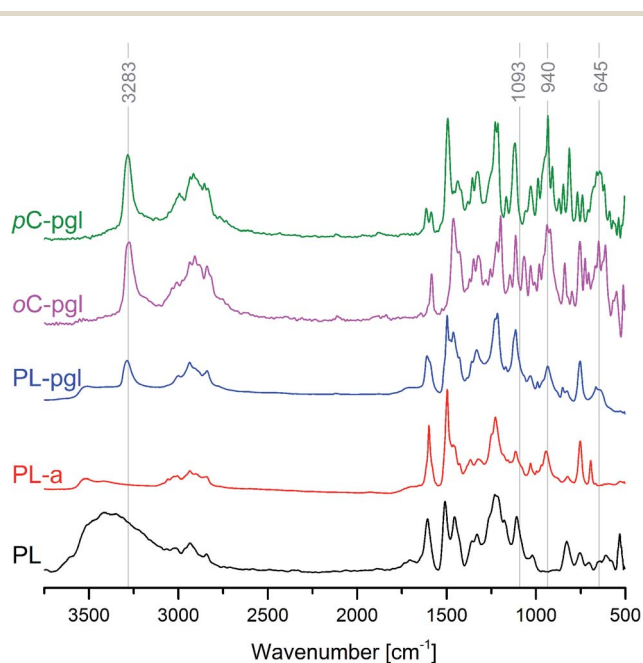


Fig. 7 FT-IR spectra of phenolated lignin PL, benzoxazines PL-a and PL-pgl as well as model compounds *o*C-pgl and *p*C-pgl showing peaks for benzoxazines ( $940 \text{ cm}^{-1}$ ) and terminal propargyl ( $645$  and  $3283 \text{ cm}^{-1}$ ).

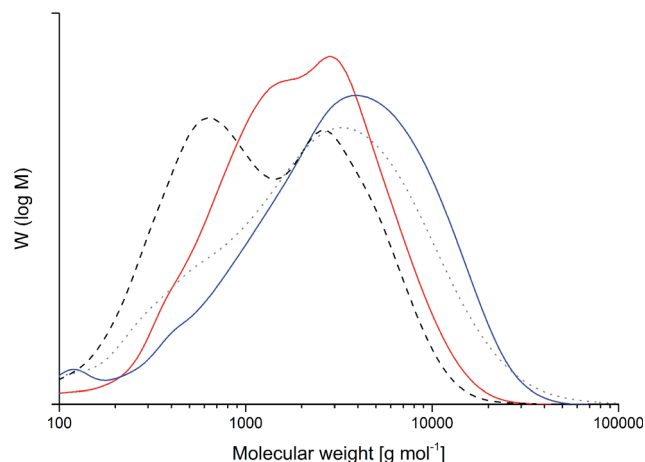


Fig. 8 Molecular weight distributions of raw (dotted gray) and phenolated lignin (dashed black) as well as benzoxazines PL-a (red) and PL-pgl (blue).

Beyond spectroscopic parameters, the change in molecular weight distribution was also investigated (Fig. 8). The weight average molecular weights were determined to be  $2200 \text{ g mol}^{-1}$  for PL,  $2900 \text{ g mol}^{-1}$  for PL-a, and  $5300 \text{ g mol}^{-1}$  for PL-pgl. The molar-mass dispersities are 2.8, 2.3 and 3.0, respectively. An increase in the molecular weights of both lignin-benzoxazines is expected due to the addition of benzoxazine units in the lignin skeleton. The theoretical values,  $3600 \text{ g mol}^{-1}$  for PL-a and  $2900 \text{ g mol}^{-1}$  for PL-pgl, are derived from the calculated  $\text{C}_9$ -unit weights of  $340 \text{ g mol}^{-1}$  for PL,  $550 \text{ g mol}^{-1}$  for PL-a and  $450 \text{ g mol}^{-1}$  for PL-pgl ( $\text{C}_9$  of plain lignin about  $200 \text{ g mol}^{-1}$  and 1.8 phenols per  $\text{C}_9$ ). The variation in the experimental values of PL-a (*i.e.* lower than theoretical) and PL-pgl (*i.e.* higher than theoretical) might be associated with different  $\text{p}K_{\text{a}}$  values of both amines. The stronger basicity of propargylamine might have resulted in more intense condensation reactions such as with formaldehyde, whereas weak basicity might predominantly have resulted in ether cleavage.<sup>46</sup> Alternatively, a small fraction of the propargyl units might have polymerized already during synthesis of benzoxazines.

Overall, it can be concluded that the product characteristics were largely attributed to the formation of benzoxazines.

### 3.3 Polymerization behavior of lignin-based benzoxazines

The polymerization process of PL-a and PL-pgl was investigated through the *in situ* FT-IR spectra shown in Fig. 9, wherein characteristic absorptions of benzoxazines (around  $940 \text{ cm}^{-1}$  and  $1227 \text{ cm}^{-1}$ )<sup>8</sup> quickly disappeared, indicating the opening of benzoxazines rings. This rather fast polymerization at  $180 \text{ }^\circ\text{C}$  is catalyzed by the existing phenolic groups acting as benzoxazine polymerization catalyst. The presence of a small amount of phenolic groups is evident by the broad bands in the range  $3300\text{--}3600 \text{ cm}^{-1}$  in the FT-IR spectra of PL-a and PL-pgl.

In PL-pgl, the signals referring to propargyl structures ( $3283 \text{ cm}^{-1}$  and  $645 \text{ cm}^{-1}$ )<sup>43,44</sup> vanished because propargyl units have also polymerized. This thermally activated reaction is reported to result in cyclotrimerization of three ethynyl end groups to



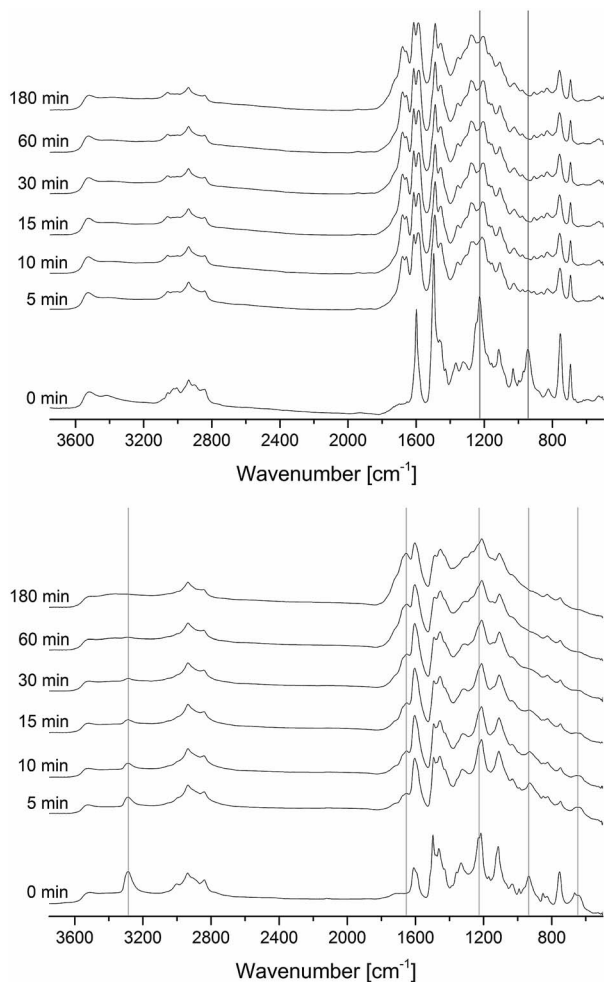


Fig. 9 *In situ* FT-IR spectra of PL-a (top) and PL-pgl (bottom) during the polymerization at 180 °C.

form a stable benzene ring, which might be indicated by the peak at  $1657\text{ cm}^{-1}$ .<sup>47,48</sup> The cyclotrimerization can lead to crosslinked structure in addition to the polymerization due to the multiple benzoxazine groups in the lignin molecule. According to Demir *et al.* the cyclotrimerization usually occurs around or above 220 °C.<sup>44</sup> However, this process is known to be responsive to a wide range of catalysts. The rich functionality of lignin possibly induced a catalytic effect causing the polymerization to occur at a lower temperature, *i.e.* at isothermal heating temperature of 180 °C. From the *in situ* FT-IR spectra in Fig. 9 it can be seen that the polymerization of PL-a continued for 30 min, and of PL-pgl for 60 min. In both samples, only minor changes occurred afterwards until 180 min.

The polymerization process of lignin–benzoxazines and model benzoxazine compounds was additionally monitored by DSC (Fig. 10), and compared to BA-a in Table 1, a basic benzoxazine structure widely regarded as the standard benzoxazine monomer, which is derived from bisphenol-A and aniline. BA-a was used previously with regard to benzoxazine–lignin blends.<sup>17</sup> By directly using lignin to synthesize the benzoxazine PL-a, the onset and maximum polymerization temperatures were similarly low as compared to the blend of BA-a and lignin

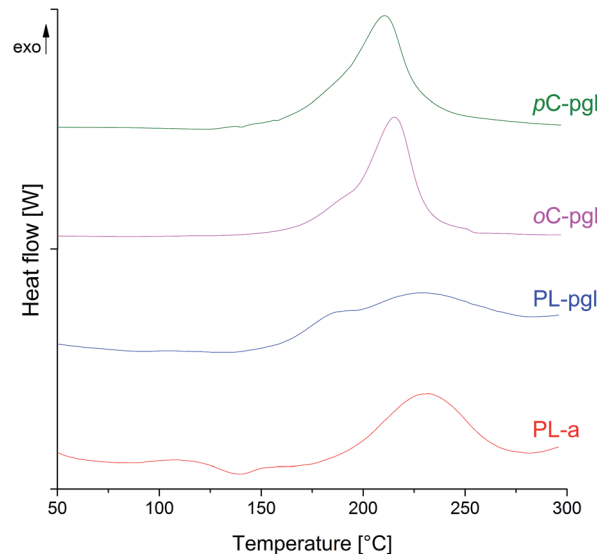


Fig. 10 DSC thermograms of lignin–benzoxazines and model compounds (y-axes for the two sets were scaled differently, see Table 1 for enthalpy integrations).

reported by El Mansouri *et al.*<sup>17</sup> In the previous studies, it was recognized that acidic hydroxyl groups, which were also present in PL, catalyzed the polymerization processes.<sup>49</sup> However, the catalytic effect was more prominent for blends than lignin-based benzoxazines. This observation could be attributed to the reduction of hydroxyl groups in the latter during formation of oxazine rings (except 5-substituted units).

In the polymerization of propargyl benzoxazines (Fig. 10), two exothermic signals were recorded. The smaller exotherm occurring at a slightly lower temperature was attributed to the polymerization of propargyl groups while the larger exotherm corresponded to the polymerization of benzoxazines. All three propargyl benzoxazines showed similar polymerization temperatures (Table 1), with PL-pgl having lower onset (*i.e.* for polymerization of both, propargyl and benzoxazine groups) and higher maximum temperature (*i.e.* for polymerization of benzoxazine groups).

In quantification of DSC signals, lignin-based benzoxazines showed significantly lower enthalpies of polymerization ( $\Delta H$  in Table 1) compared to the two model benzoxazine compounds despite having the same end-capping moieties, an indication of the lower benzoxazine density in the former. This was attributed to the inherent oligomeric nature of lignin, which was less saturated with phenols qualified for the formation of benzoxazine rings, *i.e.* in comparison to the phenols used for the synthesis of the model benzoxazine compounds. In addition, the higher enthalpy of polymerization for PL-pgl compared to PL-a was due to the cyclotrimerization of ethynyl groups.

The characterization of thermal stability by TGA (Fig. 11) revealed that onset temperatures of the decomposition reactions were largely comparable (Table 1). Only the lignin-free reference BA-a and the phenolated lignin PL decomposed earlier. A similar trend was observed for the maximum temperatures of decomposition.



**Table 1** Summary of polymerization and degradation temperatures ( $T_p$  and  $T_d$ , respectively; temperatures for propargyl polymerization in brackets) as well as char content and limited oxygen index (LOI)

	$T_{p,onset}$ [°C]	$T_{p,max}$ [°C]	$\Delta H$ [J g <sup>-1</sup> ]	$T_{d,onset}$ [°C]	$T_{d,max}$ [°C]	Char [% , 800 °C]	LOI
PL	—	—	—	292	358	17.3	24.4
BA-a <sup>a</sup>	249	261	277	268	299	25.7	27.8
BA-a-SL (7 : 3) <sup>a</sup>	176	212	303	316	375	40.8	33.8
PL-a	190	230	117	328	424	47.5	36.5
PL-pgl	154 (156)	225 (185)	224	329	419	51.9	38.3
<i>o</i> C-pgl	185 (165)	215 (188)	1130	326	401	28.3	28.8
<i>p</i> C-pgl	175 (161)	210 (184)	1192	329	401	31.5	30.1

<sup>a</sup> Bisphenol-A/aniline benzoxazine (BA-a) with rice straw soda lignin (SL) as published by El Mansouri *et al.*<sup>17</sup>

In a review on lignin thermal degradation properties, a multitude of lignins showed maximum decomposition temperatures mostly around 360 °C (ranging from about 240 °C to 390 °C),<sup>50</sup> which are in good agreement with PL. Among all samples, benzoxazines synthesized from lignin had the highest temperature maxima at 419 °C and 424 °C and thus the highest thermal stability. For lignin-based epoxy resins, a comparable high decomposition temperature of 416 °C was also found in literature.<sup>51</sup>

As another measure for thermal stability, the amount of char formation was studied at 800 °C (Table 1). For both lignin-based benzoxazines, the char formation was approximately three times higher than for phenolated lignin alone; and approximately two times higher than those of the two model compounds. With the potential formation of new benzene rings from cyclotrimerization, the char yield of PL-pgl was higher than PL-a by about 9%. The limiting oxygen index (LOI), a parameter used to evaluate the degree of flammability of materials, was calculated using the van Krevelen and Hoftyzer equation with  $LOI = 17.5 + 0.4 \times (\text{char yield})$ .<sup>52,53</sup> According to the class scheme by Nelson,<sup>54</sup> PL and BA-a were both slow burning materials ( $LOI \approx 21$  to 28). Although the suggested

criteria for self-extinguishing LOI value vary depending on the literature, the material with LOI values greater than 28 were proposed to be self-extinguishing by Fenimore<sup>55</sup> and Nelson.<sup>54</sup> Under this criterion of self-extinguishing, both lignin-based benzoxazines in Table 1 are self-extinguishing and better than those compared. Recently, an enhanced LOI value was similarly reported when adding increasing amounts of Kraft and organosolv lignin to epoxy resins. The authors obtained a maximum LOI of 32.7, which was exceeded by the lignin-benzoxazines presented here.<sup>51</sup>

The propargyl group is known to impart good thermal stability. Both *p*C-pgl and *o*C-pgl possess higher propargyl concentration per unit molecular weight than PL-pgl. Furthermore, PL-a has no propargyl group in its monomer structure. Despite these facts, PL-a and PL-pgl showed better thermal stability. However, it should be pointed out that the two model compounds used are based on monofunctional phenolic compounds. It is well known in the literature that monofunctional benzoxazines do not polymerize into large molecular weight polymers and form small oligomers of typical molecular weight of 500–2000 g mol<sup>-1</sup>.<sup>8</sup> On the other hand, the lignin-based benzoxazines has already larger molecular size prior to the polymerization reaction. Therefore, it can be safely concluded that this significant improvement in the char yield is the synergistic combination of benzoxazine group as part of the lignin molecule, rather than the intrinsic thermal stability of the propargyl-related groups formed.

## 4 Conclusions

For the first time, the syntheses of renewable aniline- and propargylamine-benzoxazines were developed solely using organosolv lignin in its phenolated form as aromatic hydroxyl group feedstock. The structural characterization by <sup>31</sup>P, <sup>1</sup>H, <sup>13</sup>C and HSQC NMR spectroscopy in combination with elemental and FT-IR analyses showed that *p*-hydroxyphenyl and guaiacyl units were successfully converted to benzoxazine units. The density of benzoxazine units formed was similar for both amines and was determined to be as high as 3.2 mmol g<sup>-1</sup>. The characterization of the polymerization process by isothermal *in situ* FT-IR studies showed that both lignin-based benzoxazines completed polymerization in an hour or less at 180 °C. Further thermal analysis by DSC and TGA revealed comparable behavior

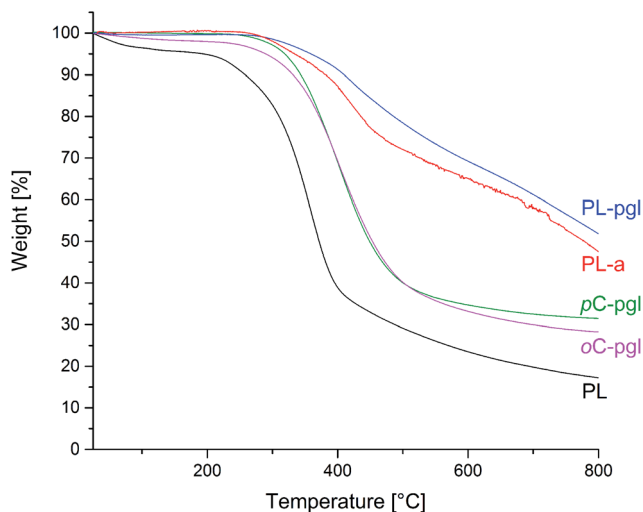


**Fig. 11** TGA thermograms of phenolated lignin PL, resulting benzoxazines PL-a and PL-pgl as well as model compounds *p*C-pgl and *o*C-pgl.



of lignin-based benzoxazines and model compounds with regard to polymerization and decomposition temperatures. The thermal stability, given by the amount of char formed during decomposition, was tremendously increased for both lignin-based benzoxazines, being three times higher than the phenolated lignin and almost two times higher than the model compounds. The propargyl-based lignin-based benzoxazine formed 9% more char than its aniline-based counterpart due to the additional benzene rings formed from cyclotrimerization of terminal ethynyl groups. Moreover, the limited oxygen indices of lignin-based benzoxazines (*i.e.* >28) led to its classification as self-extinguishing materials, pointing towards incorporation in fire retardant applications.

## Acknowledgements

One of the authors (G. J. A.) is indebted to the scholarship offered by Engineering Research and Development for Technology (ERDT) under the auspices of the Department of Science and Technology (DOST) of the Philippine government. The research was also funded by the Federal Ministry of Food and Agriculture (BMEL), and supported by the Fachagentur Nachwachsende Rohstoffe e. V. (FNR projects: Lignocellulose-Bioraffinerie II, no. 22019009 and ProLignin, no. 22020811). The authors gratefully acknowledge Rosanna Buchholz (Thünen Institute of Wood Research, TI), Andreas Schreiber (University of Hamburg), Sascha Lebioda (TI), and Christiane Riegert (TI) for their experimental and technical support.

## Notes and references

- W. O. S. Doherty, P. Mousavioun and C. M. Fellows, *Ind. Crops Prod.*, 2011, **33**, 259–276.
- S. Canas, M. C. Leandro, M. I. Spranger and A. P. Belchior, *Holzforschung*, 2000, **54**, 255–261.
- O. Anjos, C. Carmona, I. Caldeira and S. Canas, *BioResources*, 2013, **8**, 4484–4496.
- E. Adler, *Wood Sci. Technol.*, 1977, **11**, 169–218.
- Y. Lai and K. Sarkanen, in *Lignins: Occurrence, formation, structure and reactions*, ed. K. Sarkanen and C. Ludwig, John Wiley & Sons, Inc., New York, 1971, pp. 165–240.
- P. Whiting and D. A. I. Goring, *Sven. Papperstidn.*, 1981, **84**, 120–122.
- A. Tolbert, H. Akinosho, R. Khunsupat, A. K. Naskar and A. J. Ragauskas, *Biofuels, Bioprod. Biorefin.*, 2014, **8**, 836–856.
- H. Ishida, in *Handbook of benzoxazine resins*, ed. H. Ishida and T. Agag, Elsevier B.V., Amsterdam, 2011, pp. 3–81.
- C. Amen-Chen, H. Pakdel and C. Roy, *Bioresour. Technol.*, 2001, **79**, 277–299.
- T. Parsell, S. Yohe, J. Degenstein, T. Jarrel, I. Klein, E. Gencer, B. Hewetson, M. Hurt, J. I. Kim, H. Choudhari, B. Saha, R. Meilan, N. Mosier, F. Ribeiro, W. N. Delgass, C. Chapple, H. I. Kenttämaa, R. Agrawal and M. M. Abu-Omar, *Green Chem.*, 2015, **17**, 1492–1499.
- K. Chiou and H. Ishida, *Curr. Org. Chem.*, 2013, **17**, 913–925.
- N. K. Sini, J. Bijwe and I. K. Varma, *J. Polym. Sci., Part A: Polym. Chem.*, 2014, **52**, 7–11.
- E. Calò, A. Maffezzoli, G. Mele, F. Martina, S. E. Mazzetto, A. Tarzia and C. Stifani, *Green Chem.*, 2007, **9**, 754–759.
- H. Kimura, Y. Murata, A. Matsumoto, K. Hasegawa, K. Ohtsuka and A. Fukuda, *J. Appl. Polym. Sci.*, 1999, **74**, 2266–2273.
- H. Xu, Z. Lu and G. Zhang, *RSC Adv.*, 2012, **2**, 2768–2772.
- J. Podschun, B. Saake and R. Lehnen, *Eur. Polym. J.*, 2015, **67**, 1–11.
- N.-E. El Mansouri, Q. Yuan and F. Huang, *J. Appl. Polym. Sci.*, 2012, **125**, 1773–1781.
- H. M. E. Haque, Z. Islam, T. Kawauchi and T. Takeichi, *Appl. Mech. Mater.*, 2012, **217–219**, 571–577.
- T. Ougi, *et al.*, WO 2013031039 A1, 2013.
- M. Comí, G. Lligadas, J. C. Ronda, M. Galià and V. Cádiz, *J. Polym. Sci., Part A: Polym. Chem.*, 2013, **51**, 4894–4903.
- J. Podschun, A. Stücker, B. Saake and R. Lehnen, *ACS Sustainable Chem. Eng.*, 2015, **3**, 2526–2532.
- H. Ishida and H. Y. Low, *Macromolecules*, 1997, **30**, 1099–1106.
- H. Ishida and D. Allen, *J. Polym. Sci., Part A: Polym. Chem.*, 1996, **34**, 1019–1030.
- M. Kanchanasopa, N. Yanumet, K. Hemvichian and H. Ishida, *Polym. Polym. Compos.*, 2001, **9**, 367–375.
- S. W. Kuo, Y. C. Wu, C. F. Wang and K. U. Jeong, *J. Phys. Chem. C*, 2009, **113**, 20666–20673.
- A. Granata and D. S. Argyropoulos, *J. Agric. Food Chem.*, 1995, **43**, 1538–1544.
- M. Zawadzki and A. Ragauskas, *Holzforschung*, 2001, **55**, 283–285.
- E. A. Capanema, M. Y. Balakshin and J. F. Kadla, *J. Agric. Food Chem.*, 2004, **52**, 1850–1860.
- F. Tran, C. S. Lancefield, P. Kamer, T. Lebl and N. Westwood, *Green Chem.*, 2015, **17**, 244–249.
- A. Nagai, Y. Kmel, Y. Wang, M. Omura, A. Sudo, H. Nishida, E. Kawamoto and T. Endo, *J. Polym. Sci., Part A: Polym. Chem.*, 2008, **46**, 2316–2325.
- G. M. Irvine, *Tappi J.*, 1984, **67**, 118–121.
- W. Fiddler, W. E. Parker, A. E. Wasserman and R. C. Doerr, *J. Agric. Food Chem.*, 1967, **15**, 757–761.
- J. Rodrigues, J. Graça and H. Pereira, *J. Anal. Appl. Pyrolysis*, 2001, **58–59**, 481–489.
- R. Alén, E. Kuoppala and P. Oesch, *J. Anal. Appl. Pyrolysis*, 1996, **36**, 137–148.
- J. C. del Río, A. Gutiérrez, J. Romero, M. J. Martínez and A. T. Martínez, *J. Anal. Appl. Pyrolysis*, 2001, **58–59**, 425–439.
- A. I. Affi, J. P. Hindermann, E. Chornet and R. P. Overend, *Fuel*, 1989, **68**, 498–504.
- M. J. Antal Jr, *Ind. Eng. Chem. Prod. Res. Dev.*, 1983, **22**, 366–375.
- D. W. van Krevelen, in *Properties of polymers; Their correlation with chemical structure; Their numerical estimation and prediction from additive group contributions*, ed. D. W. van Krevelen and K. te Nijenhuis, Elsevier B.V., Amsterdam, 4th edn, 2009, pp. 847–873.
- H. Ishida and J. Liu, in *Handbook of Benzoxazine Resins*, ed. H. Ishida and T. Agag, Elsevier, Amsterdam, 2011, pp. 85–102.



- 40 J. M. García, G. O. Jones, K. Virwani, B. D. McCloskey, D. J. Boday, G. M. Huurne, H. W. Horn, D. J. Coady, A. M. Bintaleb, A. M. S. Alabdulrahman, F. Alsewailam, H. A. A. Almegren and J. L. Hedrick, *Science*, 2014, **344**, 732–735.
- 41 Z. Brunovska, J. P. Liu and H. Ishida, *Macromol. Chem. Phys.*, 1999, **200**, 1745–1752.
- 42 A. E. Wroblewski, C. Lensink, R. Markuszewski and J. G. Verkade, *Energy Fuels*, 1988, **2**, 765–774.
- 43 H. J. Kim, Z. Brunovska and H. Ishida, *Polymer*, 1999, **40**, 6565–6573.
- 44 K. D. Demir, B. Kiskan and Y. Yagci, *Macromolecules*, 2011, **44**, 1801–1807.
- 45 National Institute of Advanced Industrial Science and Technology, Spectral database of organic compounds, SDBS, <http://sdb.sdb.aist.go.jp>.
- 46 K. Lundquist, in *11th International Symposium on Wood and Pulp Chemistry*, Nice, France, 2001, pp. 1–4.
- 47 M. J. Lambregts, E. J. Munson, A. A. Kheir and J. F. Haw, *J. Am. Chem. Soc.*, 1992, **114**, 6875–6879.
- 48 P. Pichat, J. Vedrine, P. Gallezot and B. Imelik, *J. Catal.*, 1974, **32**, 190–203.
- 49 D. A. I. Goring, in *Lignins: occurrence, formation, structure and reactions*, ed. K. V. Sarkanen and C. H. Ludwig, Wiley-Interscience, New York, 1971, pp. 695–865.
- 50 M. Brebu and C. Vasile, *Cellul. Chem. Technol.*, 2010, **44**, 353–363.
- 51 F. Ferdosiana, Z. Yuana, M. Anderson and C. Charles Xu, *J. Anal. Appl. Pyrolysis*, 2016, **119**, 124–132.
- 52 D. van Krevelen and P. Hoftyzer, *Properties of Polymers*, Elsevier, New York, 2nd edn, 1976.
- 53 D. W. van Krevelen, *Polymer*, 1975, **16**, 615–620.
- 54 M. I. Nelson, *Combust. Theory Modell.*, 2001, **5**, 59–83.
- 55 C. P. Fenimore, in *Flame-Retardant Polymeric Materials*, ed. M. Lewin, S. M. Atlas and E. M. Pearce, Plenum Press, New York, 1975, pp. 371–397.

